Formation of Martian Flood Features by Release of Water From Confined Aquifers

MICHAEL H. CARR

U.S. Geological Survey, Menlo Park, California 94025

Many large Martian channels arise full born from discrete areas of chaotic terrain. Estimates of peak discharges based on channel dimensions range from 10^6 to 10^8 m^3/s. It is here proposed that the large channels were eroded by water released rapidly, under great pressure, from deeply buried aquifers. Early in the planet's history the old cratered terrain was probably highly permeable to depths of several kilometers as a result of its volcanic origin and intense brecciation by meteorite impact. Extensive dissection of the old cratered terrain by fine channels suggests that fluvial action was widespread at that time and that warmer climatic conditions prevailed. Much of the water which cut the fine channels was probably removed from surface circulation and entered the groundwater system. Subsequent global cooling trapped the groundwater under a thick permafrost layer and formed a system of confined aquifers. Thickening of the permafrost and warping of the surface created high pore pressures within the aquifers, particularly in low areas. Episodic breakout of water from the aquifers could have been triggered either by impact or by the pore pressure reaching the lithostatic pressure. The rate of outflow would have depended on the aquifer thickness and permeability, its depth of burial, and the diameter of the region over which water had access to the surface. Plausible values give discharges that range from 10^5 to 10^7 m^3/s. Outflow from the aquifer probably caused undermining of the adjacent areas and collapse of the surface to form chaos. Flow ceased when the aquifer was depleted, or when the hydraulic gradient around the chaos, and thus the flow, was so reduced that the flow could freeze. The process could be repeated if the aquifer were recharged.

INTRODUCTION

Since their discovery in 1971 [*McCauley et al.*, 1972; *Masursky*, 1973; *Milton*, 1973] the channels of Mars have posed some of the most intriguing questions of Martian geology. Many of the channels resemble terrestrial fluvial features. However, liquid water is unstable under climatic conditions currently prevailing at the Martian surface. With surface temperatures that range from 150° to 300°K [*Leighton and Murray*, 1966; *Opik*, 1966; *Sinton and Strong*, 1960] and a surface pressure due largely to CO_2 in the 5- to 10-mbar range [*Leighton and Murray*, 1966; *Kliore et al.*, 1965], liquid water will rapidly evaporate or freeze depending on location, time of day, and season. Because of this problem several authors have suggested that the channels were not formed by running water but by alternative means such as lava erosion [*Carr*, 1974; *Schoenfeld*, 1977; *Cutts et al.*, 1978*a*] or a combination of tectonic and wind action [*Schumm*, 1974; *Cutts et al.*, 1976, 1978*b*]. A detailed critique of this issue is outside the scope of this paper, but most workers remain convinced that most channels were formed by running water [*McCauley et al.*, 1972; *Masursky*, 1973; *Masursky et al.*, 1977; *Milton*, 1973; *Baker and Milton*, 1974; *Hartmann*, 1974; *Sharp and Malin*, 1975; *Malin*, 1976*a*, *b*; *Pieri*, 1976; *Nummedal*, 1976; *Baker*, 1977; *Carr*, 1977]. The alternatives to water particularly fail to explain the integrated tributary networks common in the older terrains. In addition, the lack of recognizable volcanic features associated with the channels is difficult to reconcile with any volcanic hypothesis, and wind is unlikely to cause the observed universal conformity of channel direction with regional slope. If the channels were formed by water, then climatic conditions must have been different in the past, at least when the smaller channels formed [*Pollack*, 1979]. Furthermore, models of evolution of the atmosphere and the outgassing history of the planet must permit the presence of sufficient liquid water at the surface to erode the channels.

Paper number 9B0055.

CHANNEL TYPES, RELATIVE AGES, AND IMPLIED DISCHARGE RATES

A wide variety of channels occur at the surface with a range of apparent ages. *Sharp and Malin* [1975] identify three major channel types: runoff channels, fretted channels, and outflow channels. Runoff channels include the numerous channel networks and gullies that dissect much of the old cratered terrain. A simple gully is the predominant form, but many well-developed tributary systems are present. Most are probably valleys and not true channels; that is, they were never filled with water but contain a central channel. These runoff channels are generally smaller than the other two channel types noted here, being generally less than 1 km in width and up to several tens of kilometers in length. The second class of Sharp and Malin, the fretted channels, tends to be similarly restricted to the old cratered terrain. This class includes wide flat-floored channels which decrease in width upstream and which may or may not have tributaries. The origin of these channels is unclear, but mass wasting may play a major role in their development [*Carr and Schaber*, 1977; *Squyres*, 1978]. The third major class of channel identified by Sharp and Malin, the outflow channels, includes those which emerge full born from localized sources. They are broadest and deepest at their source and tend to decrease in size downstream, although this is not uniformly true. Most emerge from chaotic terrain and have features strongly suggestive of catastrophic flooding [*Milton*, 1973; *Sharp*, 1973; *Baker and Milton*, 1974; *Nummedal*, 1976; *Baker*, 1977]. The precise mechanism whereby such large flood features formed has been the subject of considerable speculation and is the main concern of this paper.

Most, but not all, outflow channels occur around Chryse Planitia. Chaotic terrain is particularly common to the south and southeast of Chryse Planitia [*Carr et al.*, 1973], where large areas of the former cratered surface have been broken into blocks along complexly intersecting fractures [*Sharp*, 1973]. The chaotic areas commonly are surrounded by an inward facing scarpment and stand 1–2 km below the sur-

Fig. 1. Typical relations between chaos and a large channel at 43°W, 2°S. A 20-km-wide channel emerges full born from a 40-km-radius area of chaos enclosed by an inward facing escarpment. Viking mosaic P-16983.

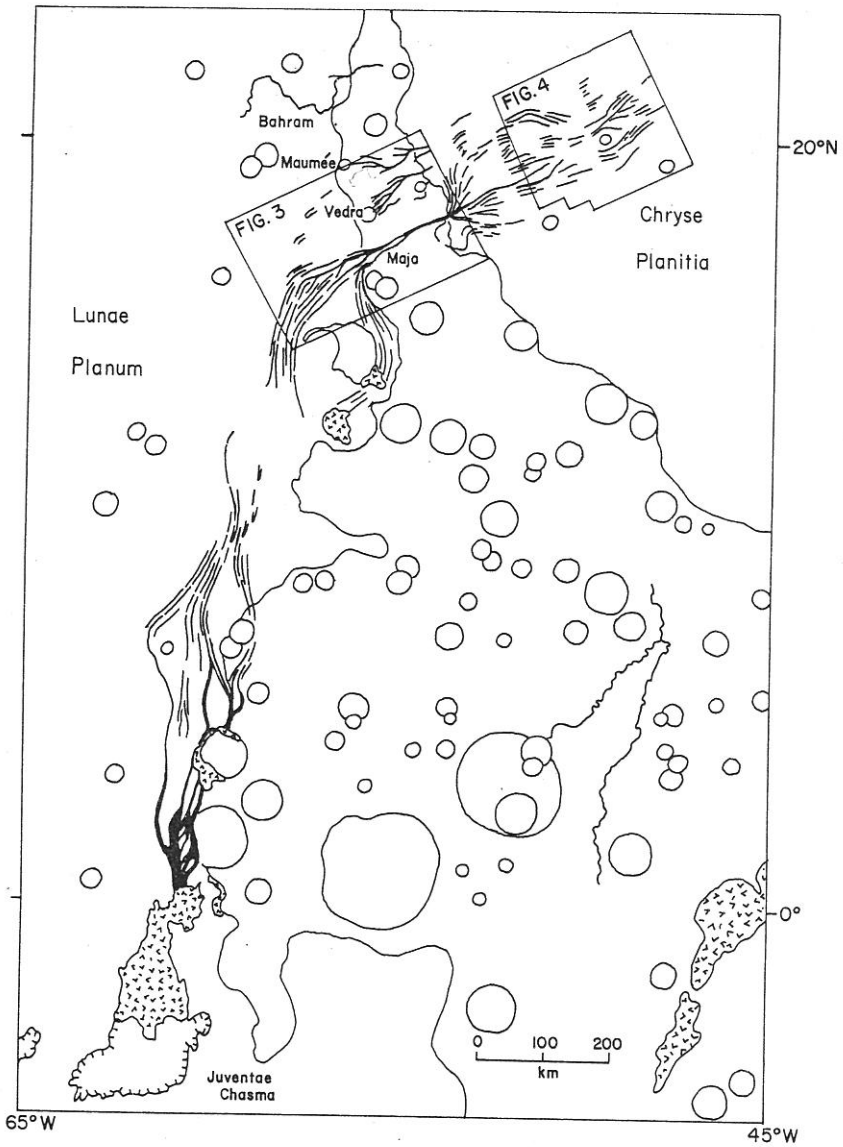

Fig. 2. Distribution of fluvial features along the eastern boundary of Lunae Planum. The flow features originate in Juventae Chasma, a depression bound by a steep inward facing escarpment and partially filled with chaos. The flow lines indicated are arrays of linear parallel grooves, tear-drop-shaped islands, and channels. Such features can be traced from Juventae Chasma northward for 1000 km and then northwest across Chryse Planitia. Chaos areas are shown in a stippled pattern.

rounding terrain [*Sharp,* 1973; *Barth et al.,* 1975]. Many areas of chaos merge with canyons as the inward facing escarpment becomes the canyon wall and the chaos merges with canyon floor deposits. The escarpment that bounds the chaos is often breached on the downslope side where a channel emerges (see Figure 1). Many outflow channels are enormous by terrestrial standards. Ares Vallis, for example, is approximately 25 km across at its source and extends for over 1000 km. Most chaos areas are irregular in outline, but some are circular and confined to the interiors of large craters. Figure 1 shows a typical example of the relationship between chaos and channels [see *Baker,* 1977; *Sharp and Malin,* 1975; *Wilhelms,* 1976]. Most chaos is within the old heavily cratered terrain. Where the old terrain is completely or partially buried by younger deposits, as at the southern end of Juventae Chasma and at the east end of Capri Chasma and Eos Chasma, the escarpment tends to be higher, and an elongate, steep-walled, and relatively flat floored canyon forms rather than typical chaos. In several areas are completely enclosed depressions with no outflow channel.

Many characteristics of outflow channels are spectacularly demonstrated by the channel system that emerges from Juventae Chasma at 62°W, 3°S (Figure 2). Juventae Chasma is a 250 × 100 km depression completely enclosed by an escarpment except to the north, where a large channel emerges. The general relation is the same as that in Figure 1 but at a much larger scale. The southern half of the chasma with its high escarpment and relatively flat floor resembles many sections of the equatorial canyon system. The northern half is filled with jostled blocks and is typical chaos. North of the chaotic area the boundary between the old cratered terrain to the east and the younger Lunae Planum to the west is extensively modified by branching channels which diverge and converge around obstacles such as low hills and craters. Longitudinal grooves, tear-drop-shaped islands, and low horseshoe-shaped escarpments can be traced along the boundary for about 1000 km

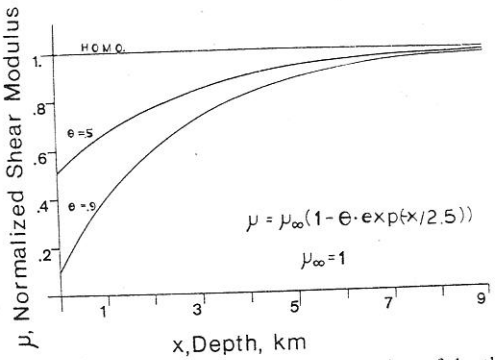

Fig. 3. Normalized shear modulus as a function of depth for the two values of the defect modulus θ used in the calculations. The straight line of the homogeneous case represents the asymptote for the varying modulus case.

$\theta = 0.5$ for laboratory data and $\theta = 0.9$ for in situ data (Figure 3). These values represent reasonable bounds for the effect of overburden on shear modulus.

We apply the general theory of the previous section, starting again from a single dislocation, to the particular law for $\mu(x)$ in (8). Substitution of (8) into (3) gives the differential equation

$$\frac{d}{dx}\left\{\mu_\infty(1 - \theta e^{-x/x_0})\frac{df}{dx}\right\} - s^2\mu_\infty(1 - \theta e^{-x/x_0})f = 0 \qquad (9)$$

Letting

$$z = \theta e^{-x/x_0}$$

in (9) yields the following differential equation:

$$z^2(1 - z)f'' + z(1 - 2z)f' - k^2(1 - z)f = 0 \qquad (10)$$

where $k^2 = s^2x_0^2$ and prime means differentiation with respect to z. *Canales* [1975] gives the two independent solutions to (10):

$$f_1 = z^k\,{}_2F_1[\tfrac{1}{2} + k + (k^2 + \tfrac{1}{4})^{1/2},$$
$$\tfrac{1}{2} + k - (k^2 + \tfrac{1}{4})^{1/2}, 1 + 2k; z]/\mu_\infty \qquad (11a)$$

$$f_2 = z^{-k}\,{}_2F_1[\tfrac{1}{2} - k + (k^2 + \tfrac{1}{4})^{1/2},$$
$$\tfrac{1}{2} - k - (k^2 + \tfrac{1}{4})^{1/2}, 1 - 2k; z]/\mu_\infty \qquad (11b)$$

where ${}_2F_1$ is the Pochhammer symbol notation of the hypergeometric function [*Arfken*, 1968]. As expected, f_1 is regular in the interval $(0, \infty)$, and f_2 in the interval $(-\infty, 0)$.

The solutions f_1 and f_2 are then used to construct the elastic fields. As can be seen, f_1 and f_2 have no dependence on the rigidity's absolute value but only on its shape through the parameters x_0 and θ in z and k.

In order to calculate the stresses produced by the screw dislocation we need to know the function $\alpha(s)$ defined by (5). The Wronskian for the solution system given by (11a) and (11b) is [*Canales*, 1975]

$$\Delta(z) = -\frac{2k}{z(1 - z)} \qquad (12)$$

and since $\Delta(x) = -(z/x_0)\Delta(z)$, we find

$$\alpha(s) = 2s \qquad (13)$$

Although the differential equation (9) can be solved in closed form giving f_1 and f_2, the actual integrals for displacement and stress could not readily be evaluated. The solution was obtained numerically using an IBM 370/168 computer.

To evaluate the displacement kernel, a Fourier sine transformation was performed using Claerbout's fast Fourier transform subroutine Fork [*Claerbout*, 1974]. The evaluation of the hypergeometric function was performed using a partial sum of the defining series [*Abramowitz and Stegun*, 1965]. The convergence of this series is extremely slow. A special technique had to be implemented to accelerate the convergence (see the appendix), and only values up to $\theta \leq 9$ could be evaluated. The singularities of f_2 for integer and half-integer values of k are cosecant singularities of alternating sign and thus canceled in the integration.

As a check of the numerical schemes, θ was set equal to 0.001 and compared with the exact results for a screw dislocation in a homogeneous medium. The worst agreement between these cases differed by less than 2%, and the usual results differed by a few tenths of a percent.

For completeness we give the equations for free-surface displacement and in-fault shear stress kernels for a single screw dislocation buried at a depth x^*. Since the rigidity is constant, the free-surface displacement is the sum of the dislocation and its image at $-x^*$:

$$w(y) = \frac{b}{2\pi}\left[\tan^{-1}\left(\frac{y}{x - x^*}\right) - \tan^{-1}\left(\frac{y}{x + x^*}\right)\right] \qquad (14)$$

where again b is the relative slip, or Burgers vector, of the dislocation. By similar arguments the fault shear stress is the superposition of source and image:

$$\sigma_{yz} = \frac{\mu_0 b}{2\pi}\left[\frac{1}{x - x^*} - \frac{1}{x + x^*}\right] \qquad (15)$$

where μ_0 is the homogeneous shear modulus, which for the calculations is normalized to unity. These expressions are used as a basis of comparison with the varying rigidity model developed previously.

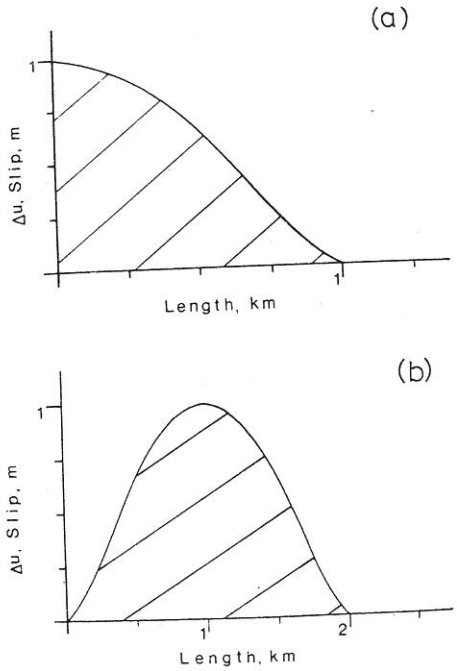

Fig. 4. Fault slip functions describing the relative offset across the fault plane as a function of depth. (*a*) Surfaced fault case. (*b*) Buried case.

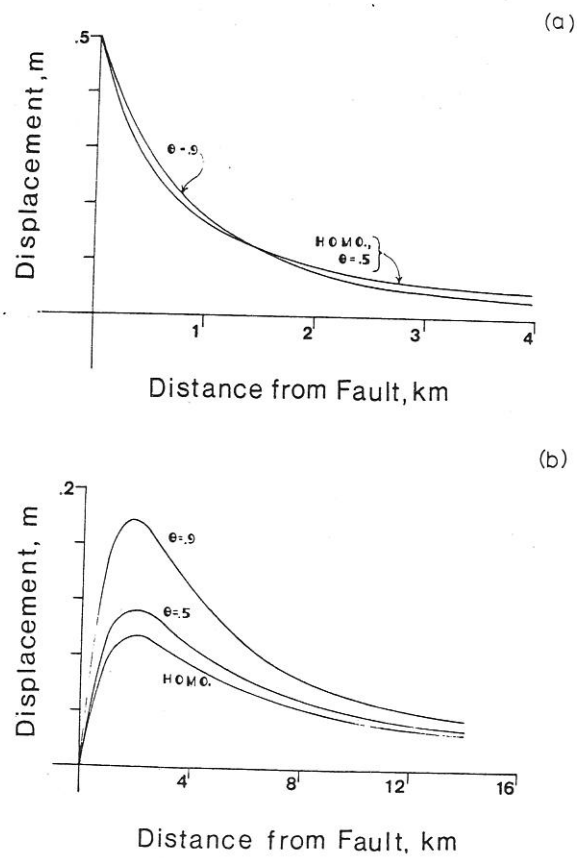

Fig. 5. Map view of typical surface displacements as a function of distance from the fault. Only displacement on one side of the fault is shown, since results are antisymmetric. (*a*) Surfaced fault case. (*b*) Buried case.

Model Parameters

Using these numerical methods for a single buried screw dislocation, finite slip zones solutions were calculated. To avoid unphysical stress singularities, the fault slip $b(x)$ had to satisfy the smooth closure conditions: (1) $b(x)$ is a continuous function for all x and (2)

$$b(x)|_{x_i,x_i+l} = \frac{db(x)}{dx}\bigg|_{x_i,x_i+l} = 0 \qquad (16)$$

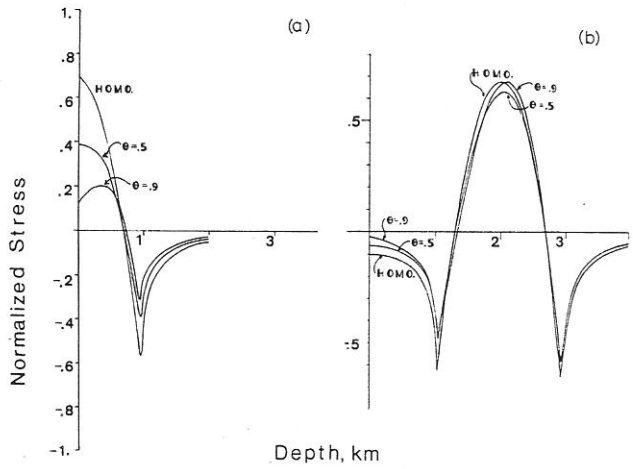

Fig. 6. Typical change in fault shear stress (normalized) as a function of depth. (*a*) Surfaced fault case. (*b*) Buried case.

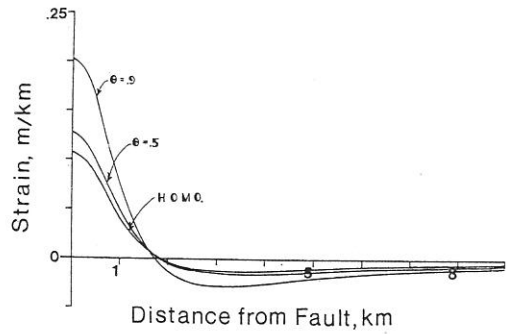

Fig. 7. Map view of typical surface strains as a function of distance from the fault. The strain on one side of fault is shown, since strain field is symmetric. Since surface strains are practically independent of modulus for the surfaced fault case, only the strains for the buried fault are given.

where x_i is the nonzero depth from the free surface to the leading edge of the fault and l is the length of the fault.

Two general classes of faults were examined: those which broke the surface, smoothly reducing to zero slip at some depth; and those faults which were completely buried, with smooth closure at both upper and lower ends. All slip zones for buried faults were 2 km long. All slip zones for surfaced faults were 1 km deep.

For convenience the maximum offset for each slip zone was set equal to 1 m, and the asymptotic modulus μ_∞ was normalized to unity. The resulting units of displacement, meters, are then the same as the units of the fault offset, while units of stress are dimensionless.

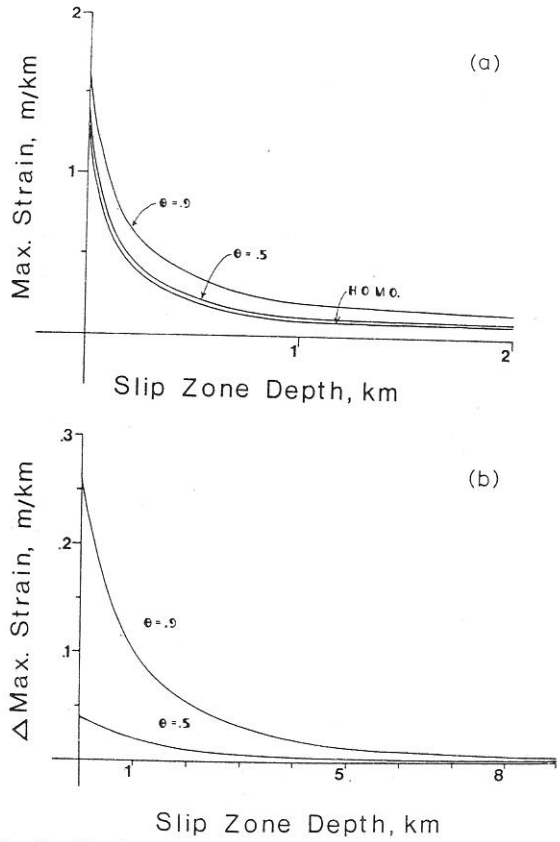

Fig. 8. Maximum or peak strain (normalized) calculated at fault trace as a function of fault depth. Fault depth is measured to edge of the slip zone closest to the surface for the buried case. (*a*) Results for all three crust models. (*b*) Results after the homogeneous results have been subtracted out.

densely cratered terrain is almost everywhere dissected by small channels, at least in the equatorial regions. In contrast, the younger plains of Chryse Planitia are totally undissected by runoff channels, although they are extensively modified by outflow channels. Clearly, formation of the present Chryse Planitia surface occurred after most runoff channels formed and before most outflow channels. Flooding may have been repetitive, but the evidence is ambiguous. Where transection relations occur between different features it is unclear whether the separation of events was days or millions of years. All give similar crater counts, but the errors on the crater ages are of the order of hundreds of millions of years.

The discharges required to form the large channels cannot be estimated with any confidence, mainly because of the uncertainty in the depth of water at the flood peak. Channel depths give only a maximum depth for the water; a channel 1 km deep can be cut by water 1 m deep, given sufficient time. However, estimates of discharge were made by making several assumptions about depth and applying the well-known Chézy-Manning formula [*Chow,* 1959], adapted for Mars gravity:

$$Q = \frac{0.51}{n} AR^{2/3}\theta^{1/2} \quad (1)$$

where Q is the discharge in meters per second, A is the cross-sectional area of the channel, n is the roughness coefficient, R is the hydraulic radius, and θ is the slope. In several places on Lunae Planum the flood appears to have been diverted around ejecta ramparts. Shadow measurements suggest that these range in height up to 200 m (D. G. W. Arthur, personal communication, 1978]. The depth in these areas was then probably less than 200 m. At the other extreme, depths of several meters are likely to be required to cause the deep scour of the Lunae Planum surface. The scoured region of Lunae Planum ranges from 50 to 80 km wide (Figure 2). From these figures a probable range for the peak discharge can be calculated. Taking a slope of 0.02 [*U.S. Geological Survey,* 1976] and a roughness coefficient of 0.03 [see *Chow,* 1959, pp. 115–123], a depth of 100 m and a width of 80 km give an estimated discharge of 5×10^8 m³/s. For a 10-m depth and a 50-km width the discharge is 7×10^6 m³/s. Similar values are found for Ares Vallis, which has a slope of 0.01 and a width of 25 km. If the water was 100 m deep, the Manning formula gives a discharge of 1×10^8 m³/s; for a 10-m depth the discharge is 7×10^6 m³/s. Thus the probable range for peak discharge is 7×10^6 to 5×10^8 m³/s.

The only terrestrial channels of comparable size occur in the channeled scablands of eastern Washington. These are believed to have formed by catastrophic flooding during the rapid draining of Lake Missoula in the late Pleistocene. According to *Baker* [1973] the flood lasted only a few days, during which a peak discharge of 2.1×10^7 m³/s was achieved. *Baker and Milton* [1974] and *Baker* [1977] have made a detailed comparison of the Martian and eastern Washington channels. They point out that the Martian and terrestrial examples have many features in common, including tear-drop-shaped islands, longitudinal grooves, terraced margins, angular channel floor depressions, and inner channel cataracts. The commonality leads them to conclude that the Martian channels are indeed true channels and that they were formed by catastrophic floods. This conclusion is consistent with their general lack of tributaries and the emergence of the channels full born.

The cause of these great floods is not known, although several mechanisms have been proposed. *McCauley et al.* [1972] and *Masursky et al.* [1977] suggested that the floods are glacial bursts caused by volcanic eruptions under glaciers. Such bursts, termed jokulhlaups, are common on Iceland, where flow rates up to 10^5 m³/s are achieved [*Thorarinnsson,* 1957]. There are several problems with this mechanism. There is abundant circumstantial evidence of ground ice on Mars (see below) but relatively little evidence for surface glaciers outside the polar regions. The highest discharge that *Thorarinnsson* [1957] noted for an Icelandic glacial burst is 10^5 m³/s. Eruption into ground with interstitial ice or even large ice lenses should be much less efficient at producing floods than eruption into a glacier, and yet the discharges for the Martian cases are higher than they are for jokulhlaups. However, the main problem with this mechanism is the lack of any evidence for contemporaneous volcanic activity in the source regions, yet contemporaneous lava flows or other volcanic constructs should be highly visible because of their relatively young age and because of the contrast with the fluvial and chaotic surface morphologies. Another suggestion is that floods result as a consequence of dissociation of a CO_2-H_2O clathrate stored close to the Martian surface [*Milton,* 1974]. The phase diagram of the clathrate is such that its dissociation is pressure sensitive. The clathrate is stable, for example, at 10°C under pressures of several tens of bars but is unstable at temperatures greater than 0°C under millibar pressures. Release of pressure by some tectonic event could then trigger dissociation of the clathrate and release massive amounts of water. The heat of dissociation is derived by cooling the host rock from its initial temperature down to 0°C, when the reaction will shut itself off. This mechanism does not therefore require volcanism to supply the heat needed. However, because of the contrasting specific heats of clathrate and rock, the reaction will rapidly turn itself off if more than 1% clathrate is present, and this is barely sufficient to generate floods. Furthermore, the mechanism requires a relatively high and narrow range of mean surface temperatures (0°–10° C) for it to occur. Several authors have talked in very general terms of release of water stored underground [*McCauley et al.,* 1972; *Sharp and Malin,* 1975; *Baker,* 1977]. This paper examines the requirements for rapid release of stored water and proposes a specific mechanism for achieving them.

Formation of Confined Aquifers

The specific mechanism proposed here for forming the flood features is as follows. The rocks within several kilometers of surface are probably volcanic or brecciated by impact and thus highly porous. Very early in the planet's history, water was available at the surface to dissect the old cratered terrain, as evidenced by the numerous fine channels. Temperatures were therefore probably warmer, and the atmosphere thicker than at present. It is postulated that much of this water was lost to a groundwater system. Later the mean annual temperature fell, and a permafrost layer developed and thickened with time. Ultimately, the permafrost layer became so thick that it effectively sealed in the underlying groundwater to form a system of confined aquifers. Pressure within the aquifers would depend on their relief, but in addition, because of the volume increase of water upon freezing, an increase in depth of the base of the permafrost could add to the pore pressure within the aquifer. With progressively colder temperatures, pore pressures continued to rise. When pore pressures reached the lithostatic pressure, the aquifers became unstable. Further freezing resulted in uplift of the overlying terrain, fracturing, and breakout. Breakout could also have been triggered by meteor-

ite impact. Once access to the surface was achieved, water was forced out at rates dependent on hydraulic head, the transmissivity, the dimensions of the aquifer, and the breakout area. Flow terminated when drawdown around the breakout area so reduced flow that the water froze and resealed the aquifer. The rest of the paper examines this mechanism in detail.

The dissection of the old cratered terrain by numerous small channels and gullies attests to the very early availability of water on the Martian surface. The lack of dissection of younger features such as the sparsely cratered plains and volcanoes suggests that conditions changed relatively early, probably billions of years ago, and that fluvial activity was rare for most of the planet's history [*Malin,* 1976*b*; *Pollack,* 1979]. The present low temperatures and the thin atmosphere suggest that possible causes for the decrease of fluvial activity were loss of water from the atmosphere, a planet-wide cooling, and/or loss of an earlier, more dense atmosphere. *Owen and Biemann* [1976], *McElroy et al.* [1977], and *Anderson and Owen* [1977] have argued, primarily on the basis of the abundance of ^{36}A, that several tens of meters of water averaged over the whole surface have outgassed from the planet. This is approximately a factor of 20 less than that anticipated if Mars had comparable volatile inventory and degree of outgassing to those of the earth [*Fanale,* 1976]. Although water may have been lost from the atmosphere by chemical combination with regolith materials, by freezing out at the poles, or by loss to space, much of the water may also have been rapidly removed from atmospheric circulation by entry into the general groundwater system.

Conditions on Mars very early in its history probably favored a groundwater system of substantial capacity. At this time most of the planet's surface was almost certainly covered by densely cratered terrain, which now survives over only half the surface. Like the lunar highlands the cratered terrain is probably highly brecciated by impact to depths of many kilometers. The porous, brecciated materials may in places be interbedded with or partially covered by volcanic flows [*Malin,* 1976*a*]. Such a sequence is likely to have relatively high porosities and permeabilities. To explain the seismic transmission characteristics of the lunar surface, *Latham et al.* [1971] propose that near-surface lunar materials are loosely consolidated and that the seismic velocities increase with depth because of self-compaction which continues to depths of about 25 km. The heavily cratered surfaces of Mars probably have similar characteristics, although the higher gravity would cause self-compaction at shallower depths. Additional evidence for highly porous near-surface materials comes from the morphology of the small channels. Many disappear very abruptly. Indeed this is almost a general characteristic of small channels in the old terrain. Possible explanations are burial by younger deposits or cessation of flow caused by either evaporation or seepage into the surface. In several places, channels terminate abruptly and then reappear some distance away. Nirgal Vallis and an unnamed channel adjacent to Hadriaca Patera are prominent examples. Such relations are common in karst and volcanic regions of the earth and are strongly indicative of underground drainage. It is possible therefore that at the time the small channels formed, the surface materials were highly porous and could act as a sink for water derived either from the surface or directly by outgassing.

The depth to which porosity persists is not known. As indicated above, significant seismic scattering persists to depths of 25 km on the moon, although such scattering could be achieved with very small porosities. On the earth, water is encountered in mines and tunnels to depths in excess of 1–2 km, and some wells produce oil at depths of 6 km. Nevertheless, excavations far below the surface generally encounter little water [*Samuelson,* 1965]. It appears that on the earth, porosity generally decreases to near zero at depths of several kilometers. On Mars, by virtue of g intermediate between the earth and the moon the base of the porous layer should be in the 10- to 20-km range. Materials with the highest porosity should, however, be close to the surface.

The evidence for ground ice on Mars, although indirect, is substantial and will not be reviewed in detail here because of extensive treatment elsewhere [*Gatto and Anderson,* 1975; *Anderson et al.,* 1973; *Belcher et al.,* 1971; *Wade and de Wys,* 1968; *Salisbury,* 1966; *Sharp et al.,* 1971; *Sharp,* 1973; *Carr and Schaber,* 1977; *Soderblom and Wenner,* 1978]. Recent Viking orbiter photography adds significant support to the ground ice hypothesis. The evidence is mainly from mass-wasting features, possible thermokarst topography, patterned ground, the characteristics of many fluvial features, and the morphology of ejecta around large impact craters [*Carr and Schaber,* 1977]. Whether extensive ground ice was present early in the planet's history when dissection of the uplands occurred is not clear, but also the point is not important to the hypothesis being presented here. What is important is that following dissection of the uplands a general global cooling took place, and as a consequence the thickness of the permafrost layer increased. *Soderblom and Wenner* [1978], on the basis mainly of recurring escarpment heights, suggest that the depth to the base of the permafrost was 1–2 km throughout much of Mars' geologic history. In addition, *Fanale* [1976] has shown that the current mean annual surface temperatures imply that the 273°C isotherm is at a depth of 1 km at the equator and several kilometers at the pole, for plausible values of the internal heat flow. The global cooling may have resulted in trapping water within the brecciated upper few kilometers of the old cratered crust to form a system of confined aquifers. The upper seal was a thick permanent ice layer, and the lower seal was created by self-compaction of the rock materials.

AQUIFER PORE PRESSURE

Pore pressure is a major factor in controlling the discharge rate from confined aquifers. If the hydrostatic head within the aquifer exceeds the depth of burial, then water will flow to the surface, given an appropriate conduit. If the pore pressure is extremely high and exceeds the lithostatic pressure, then the overlying terrain will be uplifted to balance the confining pressure against the pore pressure. If the overlying seal is ruptured, water will gush to the surface under great pressure, and the overlying terrain will collapse. One important factor controlling pore pressure is the vertical relief of the aquifer, which in the Mars case would largely be controlled by surface relief, since the base of the permafrost layer and the base of the permeable zone will tend to follow the low-frequency component of surface relief. The chaotic regions around Chryse Planitia are at a lower elevation than the surrounding terrain, and the upper surface of the permeable zone must be at a correspondingly lower elevation. Thus, if the permeable zone is continuous and saturated, then an artesian system would exist with groundwater in the Chryse region under considerable hydrostatic head. The Hydraotes, Hydaspis, and Aram regions of Chaos at the heads of the Simud, Tiu, and Ares valles stand at an elevation of 4–5 km lower than cratered terrain at the eastern boundary of Lunae Planum, approxi-

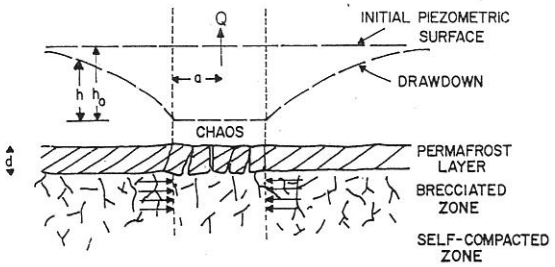

Fig. 5. Model of the proposed flood mechanism. Water is sealed under high pressure within the brecciated old cratered terrain by a permafrost layer above and compacted nonporous rocks below. Disruption of the permafrost layer in chaos regions provides access for the water to the surface. Flow into the chaos region and out onto the surface causes drawdown of the pore pressure in the region surrounding the chaos. The rapid flow causes undermining of the surface and collapse to enlarge the chaos area.

mately 1800 km to the west. Again assuming continuity, the 4- to 5-km hydrostatic head is sufficient of itself to exceed the lithostatic pressure in the chaos regions, for an aquifer buried 1–1.5 km deep.

Lowering the base of the permafrost and progressive freezing of the trapped groundwater during the period of global cooling may also have contributed to the pore pressure within the aquifer. The efficiency of this mechanism cannot be calculated because it depends on the degree to which the voids in the porous layer are water filled. If all voids are completely filled and the aquifer is sealed, then any increase in the depth of permafrost will cause rapid rise in pore pressure because of the 11% increase in volume of water on freezing and the low compressibility of water and rock materials. Under these conditions the mechanism is very efficient; for a 3-km-thick aquifer the pore pressure will increase approximately 1 bar for every 1-m increase in depth of the permafrost. These conditions would, however, be achieved only in rare circumstances, if at all. A more likely situation is that the void space is only partially filled with water. The volume change on freezing would then be accommodated by compressing the gas in the voids, and only a small rise in pore pressure would result.

CALCULATION OF DISCHARGES

We have established the possibility of an extensive water-charged layer beneath the permafrost and demonstrated mechanisms whereby water within the layer could be brought to high pressures, and possibly up to the lithostatic pressure. The remaining step is to determine if the discharge rates comparable to those implied by the scale of the channels (10^6–10^9 m^3/s) are possible from a confined aquifer.

The basic equation for flow through a confined aquifer is

$$\nabla^2 H = \frac{1}{\nu} \cdot \frac{\partial h}{\partial t} \tag{2}$$

where h is the hydrostatic head, t is the time, and ν is the hydraulic diffusivity [*Deju,* 1971; *De Wiest,* 1969]. We will attempt to solve this equation for an inifinite aquifer of uniform transmissibility and uniform compressibility which at time $t = 0$ gains access to the surface through a conduit of radius a. The problem is analogous to that of drilling a well into a confined aquifer. For this purpose, (2) can be restated in terms of drawdown around the conduit:

$$\nabla^2 w = \frac{1}{\nu} \cdot \frac{\partial w}{\partial t} \tag{3}$$

where the drawdown w is $h_0 - h$, where h_0 is the hydrostatic head at $t = 0$ and h is the head at any position (x, y) and time t (Figure 5). Equations (2) and (3) are exactly analogous to the basic heat flow equation, the thermal diffusivity being substituted for ν and temperature for w. *Carslaw and Jaeger* [1959, p. 336] provide solutions for a heat flow problem analagous to the drawdown of the hydrostatic head around a conduit to the surface in a confined aquifer. They give solutions for an infinite plate, initially at temperature T and bound internally by a hole maintained at 0°C. Solutions show the temperature profile within the plate as a function of time, radial distance, hole diameter, and diffusivity. These heat flow solutions were transposed into solution for flow in a confined aquifer by appropriate choice of the hydraulic diffusivity ν (Figure 6). The method is similar to that used by *Jacob and Lohman* [1952] to calculate discharge from a well:

$$\nu = T/S \tag{4}$$

where S is the storage coefficient and T is the transmissivity, and

$$S = \rho g b(\alpha + m\beta) \tag{5}$$

where ρ is the water density, g is the acceleration due to gravity (371 cm/s^2), b is the thickness of the aquifer, α is the vertical compressibility of the aquifer skeleton, m is the porosity, and β is the compressibility of water [*Deju,* 1971; *De Wiest,* 1969]. Values of 2×10^{-13} cm^2/dyn for α [*Clark,* 1966], 4×10^{-11} cm^2/dyn for β [*Hodgman et al.,* 1957], and 0.1 for m where used in all calculations. For a confined aquifer, flow is relatively insensitive to the value of S, which is likely to have a fairly narrow range of values as compared with T. Once the aquifer behaves as an unconfined system, however, the value of S increases substantially, and flow is greatly reduced.

The main uncertainty is in the value of the transmissivity T:

$$T = k\rho g b/\mu \tag{6}$$

where k is the permeability and μ the viscosity. Geologic materials have a wide range of permeabilities from values of 10^{-7} darcies for chert to values in excess of 3000 darcies for basalt [*Davis,* 1969]. The highest measured natural permeabilities are in sequences of basaltic lava. In the Snake River Plains basalts, transmissivities as high as 1.9 m^2/s have been calculated in a bed approximately 76.2 m thick [*Robert-*

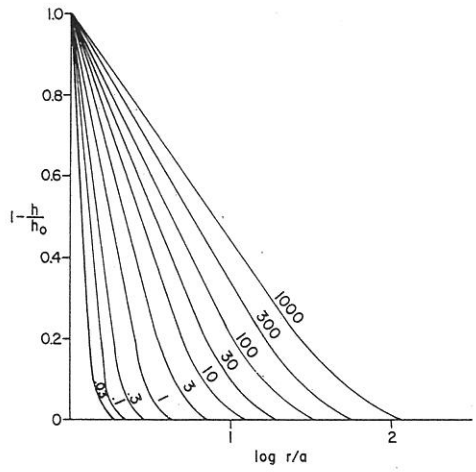

Fig. 6. Hydrostatic head around the chaos as a function of distance r from the center of the chaos and the chaos radius a for various values of $\nu t/a^2$ (adapted from *Carslaw and Jaeger* [1969, Figure 41]).

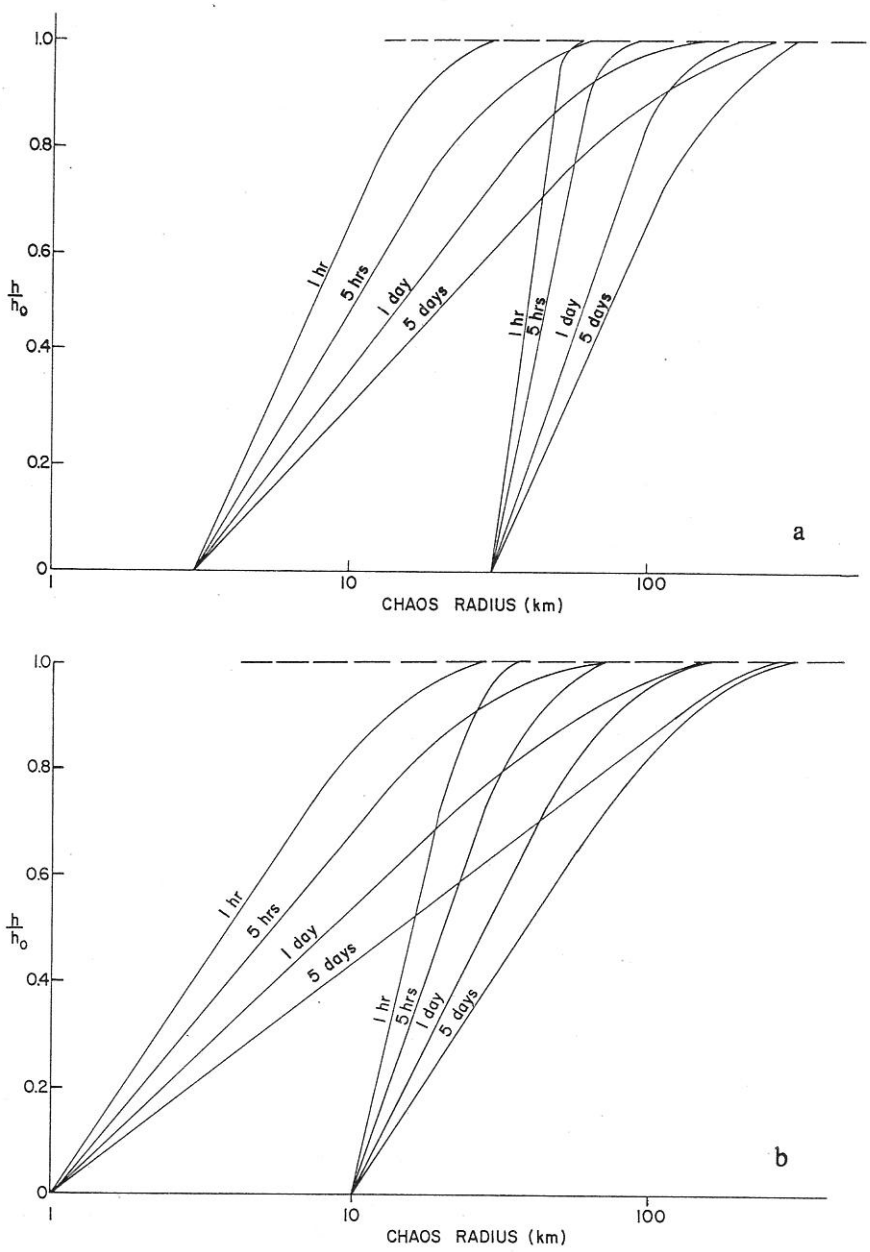

Fig. 7. Drawdown of the pore pressure around regions of chaos for various times after breakout. Drawdown is given in terms of the original hydrostatic head (h_0) before breakout for (*a*) 3- and 30-km chaos radii and (*b*) 1- and 10-km chaos radii.

son, 1974], which is equivalent to a permeability of about 2500 darcies. Values of a few hundred darcies are common for basalt aquifers in Hawaii [*Davis,* 1969]. One near Oahu, Hawaii, gives discharges indicative of a permeability of 3048 m/day, or 3700 darcies (R. H. Dale, personal communication, 1978). Lava flows are very plausible candidates for the Martian surface, although the extent to which their permeability would be increased or decreased by brecciation is uncertain. For calculation purposes a value of 1000 darcies was generally assumed.

Taking values of 4.4×10^{-12} for $(\alpha + m\beta)$ and 1000 darcies for k, the drawdown of the hydrostatic head within an aquifer, penetrated by a disturbed zone of various radii, was calculated from the solutions of the analogous heat flow problem [*Carslaw and Jaeger,* 1959, p. 336]. It was assumed that the disturbed zone, or chaos, represents an area where the upper permafrost seal is temporarily destroyed. The hydrostatic head in these regions therefore is equivalent to the depth of burial of the aquifer. Various values for t and the radius a of the disturbed zone were taken (Figure 7). Discharges were also calculated for various conditions (Figure 8 and Table 1). All calculations assumed that the flow will cease when the hydraulic head throughout the aquifer equals the depth of burial. When these conditions are achieved, rupture of the aquifer would cause water to be pumped just to the surface but would result in no overflow. The assumption is conservative. Situations can readily be conceived, such as breakout at a cliff face, where the total head, not just the excess, over the depth of burial drives the flow. A rock density of 3.5 gm/cm³ is assumed throughout. Discharge rates depend on time, the diameter of the chaotic region, the depth of burial, the aquifer thickness, and its permeability. Assuming breakout occurs when the pore pressure equals the lithostatic pressure, for an aquifer 1 km deep and 1 km thick with a permeability of 1000

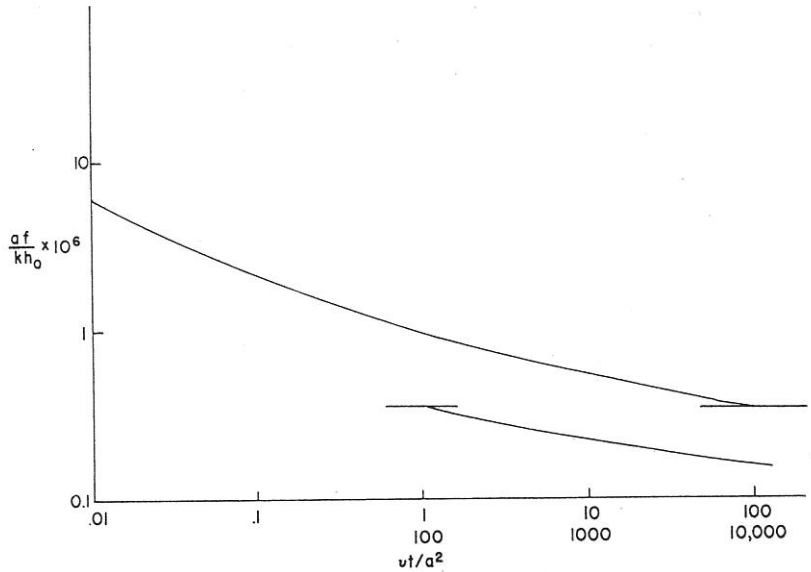

Fig. 8. The rate of flow f as a function of time. Permeability k is in darcies, and a, f, h, ν, and t are all in cgs units.

darcies, discharges range from 2.8×10^4 m³/s to 1.1×10^5 m³/s 1 hour after breakout for chaos areas 1–30 km in diameter. For an aquifer 3 km thick buried 3 km deep with a permeability of 3000 darcies, discharges after 1 hour are 1.1×10^6 to 4.2×10^6 m³/s for the same size areas. Thus the mechanism can provide discharges which approach the magnitude required, provided conditions are appropriate.

TABLE 1. Discharge Rates From a 1-km-Thick Aquifer

Time t From Breakout	Rate of Flow f, cm/s	Discharge Q, m³/s
	1-km Chaos Radius	
1 h	0.34	2.78×10^4
5 h	0.26	2.12
1 day	0.20	1.6
5 days	0.15	1.2
	3-km Chaos Radius	
1 h	0.15	3.01×10^4
5 h	0.11	2.25
1 day	0.084	1.69
5 days	0.075	1.51
	10-km Chaos Radius	
1 h	0.088	6.08×10^4
5 h	0.11	4.16
1 day	0.084	2.88
5 days	0.066	2.24
	30-km Chaos Radius	
1 h	0.056	1.12×10^5
5 h	0.036	7.13×10^4
1 day	0.022	4.5×10^4
5 days	0.017	3.4×10^4

Aquifer has a permeability of 1000 darcies, buried beneath a 1-km-thick permafrost layer. Rates are given for various values of chaos radius and time. The rate of flow f is the horizontal flow across the boundary between the aquifer and a hypothetical vertical cylinder enclosing the chaos. Discharge rates scale linearly with aquifer thickness, permeability, and depth of burial, assuming that breakout occurs when the pore pressure equals the lithostatic pressure. For example, for a 10-km chaos radius the discharge after 1 hour from a 3-km-thick aquifer, buried 3 km deep and with a permeability of 300 darcies, is $27 \times 6.08 \times 10^4$, or 1.64×10^6 m³/s.

Breakout to the surface may cause disruption of the aquifer such that in the initial high-discharge stages, part of the porous medium itself is carried along with the flow, to cause undermining and collapse of the surface. This is particularly likely if the pore pressure is at the lithostatic pressure, since the aquifer skeleton will be in part supported by the liquid. Completely enclosed depressions could thus form in the general drawdown region around the chaos areas. Undermining will also result in enlargment of the chaos area from which flow emerges so that value of a in the above equation will steadily increase. An initial chaos area, say 1 km in diameter, could expand rapidly by undermining the adjacent area. This would further supplement the discharge by a rate equivalent to the rate of engulfment of the surrounding terrain times the porosity. Table 2 shows discharges that would result for various rates of chaos enlargement. For very high enlargment rates the discharge from this mechanism will exceed the rate of flow in from the surrounding aquifer. Taking an extreme case, for a 30-km-radius area of chaos enlarging itself at a rate of 1 km/h by disrupting a 3-km-thick aquifer with 10% porosity, the discharge is 1.5×10^7 m³/s. However, such large enlargement rates are unlikely for a 30-km-radius chaos area. Erosion is likely to be extremely rapid immediately after the initial breakout, when flow velocities are very high. As can be seen from Table 1, the flow velocity decreases both with time and diameter of the conduit. Therefore as the chaos enlarges itself, the rate of enlargement probably declines. Aquifer disruption, however, probably still contributes significantly to the discharge.

Flow will terminate when it is so reduced that the water freezes and the aquifer is resealed. This could result from several causes. Drawdown around the chaos area will be relatively rapid once the drawdown region reaches the periphery of the aquifer, since the hydraulic gradient cannot be sustained by flow into the region. Thus with an aquifer of limited areal extent, shutdown will be relatively rapid. With an aquifer of infinite extent, shutdown will occur when the hydraulic gradient around the breakout region so reduces the flow that it freezes. At this time, water pressure within the aquifer could still be in excess of ρd (d being depth of burial) and fully charged with water. Another possibility is that erosion and undermining create a situation in which the face of the aquifer

TABLE 2. Discharge Resulting Directly From Chaos Enlargement by Disruption of a 1-km-Thick Aquifer

Chaos Radius, km	Volume of Water Released Per Kilometer of Enlargement, m^3	Discharge Q for Growth Rate of 1 km/h, m^3/s	Discharge Q for Growth Rate of 1 km/day, m^3/s
1	0.9×10^9	2.5×10^5	1×10^4
3	2.2×10^9	6.1×10^6	2.5×10^4
10	6.6×10^9	1.8×10^6	7.5×10^4
30	1.9×10^{10}	5.3×10^6	2.2×10^5

A porosity of 0.1 is assumed. Discharge scales linearly with aquifer thickness. Thus for a 3-km-thick aquifer breached by a 10-km-radius area of chaos enlarging itself at 1 km/day the supplementary discharge that results purely from aquifer disruption is $3 \times 7.5 \times 10^4$, or 2.25×10^5 m^3/s. This must be added to the discharge that results from flow through the aquifer to get total discharge.

is exposed at the surface. The aquifer would then no longer be confined, and water would only partially fill the voids. In this case the value of the storage coefficient S would increase rapidly, with a corresponding decrease in flow. Thus flow could terminate by different mechanisms, all ultimately resulting in freezing and resealing. The aquifer could be recharged by flow from outlying regions or by further planetary outgassing, and the cycle could then repeat itself. The water loss from the ground system with each event is so large, however, that the cycle is unlikely to be repeated too frequently.

We thus have a mechanism both for forming large floods on Mars and for terminating them. The discharges calculated for the proposed model and reasonable conditions range from 10^5 to 10^7 m^3/s, which are somewhat short of those calculated from the dimensions of the flow features (10^6–10^9 m^3/s) but not disturbingly so in view of the uncertainties. The mechanism is consistent with what is understood at present about climate change on Mars and the timing of such changes. The properties required of the near-surface materials appear reasonable in view of what is known of the early volcanic and impact history.

PREFERENTIAL LOCATION OF OUTFLOW CHANNELS IN CHRYSE REGION

The breakout mechanism may explain why much of the chaos and the flood features occur within the Chryse depression. Breakout is most likely in regions of low elevation because only there is there sufficient artesian pressure. Although increased pore pressure can be generated by freezing, generation of a head by the relief of the aquifer itself is more likely. Several areas of the Martian surface, such as Hellas, Argyre and Isidis, have negative relief but lack the chaotic terrain and breakout features. Possible explanations are that (1) in Hellas, Argyre, and Isidis a thick sequence of younger deposits overlying the old cratered terrain prevents breakout, (2) volcanic processes in the Tharsis region result in addition of water and/or other volatiles to the aquifer, thus enhancing the pore pressure, or (3) breakout is favored in the Chryse depression because the depression and the Tharsis bulge to the west formed after the aquifers. If surface temperatures were above freezing early in the planet's history, when the groundwater system was being charged, then loss of groundwater to the atmosphere would occur by seepage in low areas. Gravity data [*Phillips and Saunders,* 1975] suggest that the Chryse depression formed simultaneously with the Tharsis bulge and is younger than the other depressions. Hellas, Argyre, and Isidis, being large impact basins, probably formed very early, before global cooling, and so the groundwater system in their vicinity may have been depleted by seepage. In contrast, the Chryse depression may have formed after sealing of the aquifer system and so did not suffer a seepage loss. Although the latter explanation is somewhat speculative, the restriction of most chaos and outflow features to some of the lowest exposed areas of old cratered terrain on the planet does support the proposed breakout mechanism.

The proposed mechanism implies that the large floods occurred after global cooling. Most of the small channels such as occur widely throughout the old cratered terrain could not have formed under present climatic conditions. The small flow rates implied would result in rapid freezing and ultimately sublimation of the ice. *Lingenfelter et al.* [1968] and *Peale et al.* [1975] have shown, however, that in the case of large floods, flow can be sustained under very low temperatures and an extremely tenuous atmosphere by formation of a thick layer of surface ice which effectively insulates the interior of the flow. Thus the climatic conditions implied by the thick permafrost necessary for breakout are compatible with the flow features observed. It should be noted in passing that seepage from the aquifer system could occur after global cooling at rates sufficient to sustain flow but insufficient to cause gigantic flood features. In those cases, intermediate size channels would form.

The fate of the water is not addressed in this paper. It was postulated, however, that early in the planet's history much of the atmospheric water was lost to a groundwater system. Some fraction of this was returned to the atmosphere at a later date by the breakout mechanism. At that time, however, climatic conditions had changed drastically, and return to the groundwater system was not possible because of the thick permafrost. The water released must therefore have frozen out in the high-latitude regions or sublimed into the atmosphere to be lost to space. The volume of water involved in each episode is not known because the time over which discharge was sustained is not known. If a flood were sustained for several days, then a total discharge of 10^{10}–10^{13} m^3 would result.

IMPLICATIONS CONCERNING FORMATION OF CANYONS

The discussion above has focused on the large flood channels. The proposed breakout mechanism may have additional implications concerning the origin of the equatorial canyon system. The orientation of the canyons and many of their constituent features appear to be largely fault controlled [*Carr,* 1974; *Blasius et al.,* 1977]. However, the canyons are not simple graben. Extensive modification has taken place by mass wasting and fluvial processes, and to the east the canyons merge with chaos and large channels. Capri Chasma and Ganges Chasma, for example, merge with Simud Vallis, and the western branches of Tiu Vallis and Eos Chasma merge with Aureum Chaos. The start of the large Lunae Planum channels in Juventae Chasma has already been mentioned, emphasizing the channel-canyon connection. Any theory of origin of canyons, chaos, and channels must account for these relations. It is proposed here that some of the faulting involved in the formation of the canyon may have disrupted the postulated aquifers, causing release of water and chaos development. Water so released would have drained eastward, ultimately into Chryse Planitia. Because of the regional slope, artesian prssures would be greatest to the east, and any such release is likely to have been more voluminous there. In the higher section of the canyon to the west therefore, water may

have played an insignificant role in canyon development, whereas to the east, where high artesian pressures are likely, water may have played such a significant role that the chaos and channel characteristics dominate. As an interesting sidelight to this issue, some sections of the canyons, particularly the Ophir and Candor chasmas, are partially filled with layered deposits [*Blasius,* 1977; *McCauley,* 1979], and McCauley proposed that lakes may have once existed in the broader reaches and subsequently drained to the east.

CONCLUSIONS

1. The ancient, densely cratered terrain of Mars is highly porous, partly because of brecciation by impact and partly because of the presence of volcanic flows.
2. The porous near-surface rocks acted as a sink for the water which eroded numerous small channels early in the planet's history when climatic conditions were more temperate than the present.
3. Global cooling followed dissection of the old cratered terrain, sealing groundwater beneath a thick permafrost layer.
4. Water episodically broke out from the confined aquifers under large artesian pressures to form flood features.
5. The water which caused the floods was permanently lost from the groundwater system because the thick permafrost layer prevented reentry.

Acknowledgments. I would like to acknowledge the help of various members of the Water Resources Division of the U.S. Geological Survey, particularly J. B. Robertson, who helped me find my way in an unfamiliar field and reviewed the final manuscript. The work was supported by the Viking Project and the Planetary Geology Program, Office of Space Science, NASA Headquarters, WO-13,709.

REFERENCES

Anderson, E., and T. Owen, Mars and Earth: Origin and abundance of volatiles, *Science, 155,* 319–322, 1977.

Anderson, D. M., L. W. Gatto, and F. Ugolini, An examination of Mariner 6 and 7 imagery for evidence of permafrost terrain on Mars, in *Permafrost, The North American Contribution to the Second International Conference,* pp. 449–508, National Academy of Science, Washington, D. C., 1973.

Baker, V. R., Paleohydrology and sedimentology of Lake Missoula flooding in eastern Washington, *Geol. Soc. Amer. Spec. Pap., 144,* 79 pp., 1973.

Baker, V. R., Viking—Slashing at the Martian scabland problem, *NASA Tech. Memo., TM X-3511,* 169–172, 1977.

Baker, V. R., and D. J. Milton, Erosion by catastrophic floods on Mars and Earth, *Icarus, 23,* 27–41, 1974.

Barth, C. A., C. W. Hord, A. I. Stewart, A. L. Lane, M. L. Dick, S. H. Schaffner, and K. E. Simmons, *An Atlas of Mars: Local Topography,* University of Colorado, Boulder, 1975.

Belcher, D., J. Veverka, and C. Sagan, Mariner photography of Mars and aerial photography of Earth: Some analogies, *Icarus, 15,* 241–252, 1971.

Blasius, K. R., J. A. Cutts, J. E. Guest, and H. Masursky, Geology of the Valles Marineris: First analysis of imaging from the Viking Orbiter primary mission, *J. Geophys. Res., 82,* 4067–4091, 1977.

Carr, M. H., The role of lava erosion in the formation of lunar rilles and martian channels, *Icarus, 22,* 1–23, 1974.

Carr, M. H., Martian fluvial features, paper presented at the Eighth Meeting of the American Astronomical Society, Division of Planetary Science, Honolulu, Hawaii, Jan. 19–22, 1977.

Carr, M. H., The channels of Mars, *Sci. Amer.,* in press, 1979.

Carr, M. H., and G. G. Schaber, Martian permafrost features, *J. Geophys. Res., 82,* 4039–4065, 1977.

Carr, M. H., H. Masursky, and R. S. Saunders, A generalized geologic map of Mars, *J. Geophys. Res., 78,* 4031–4036, 1973.

Carslaw, H. S., and J. C. Jaeger, *Conduction of Heat in Solids,* 2nd ed., Clarendon, Oxford, 1959.

Chow, V. T., *Open-Channel Hydraulics,* 680 pp., McGraw-Hill, New York, 1959.

Clark, S. P. (Ed.), Handbook of Physical Constants, *Geol. Soc. Amer. Mem., 97,* 587 pp., 1966.

Cutts, J. A., K. R. Blasius, and K. W. Farrell, New data on Chryse basin landforms, *Bull. Amer. Astron. Soc., 8,* 480, 1976.

Cutts, J. A., W. J. Roberts, and K. R. Blasius, Martian channels formed by lava erosion, *Lunar and Planetary Science IX,* part 1, p. 209, Lunar and Planetary Science Institute, Houston, Tex., 1978*a*.

Cutts, J. A., W. J. Roberts, and K. R. Blasius, Chaotic terrain and channels associated with Chryse Planitia, Mars, *Lunar and Planetary Science IX,* part 1, pp. 206–209, Lunar and Planetary Science Institute, Houston, Tex., 1978*b*.

Davis, S. N., Porosity and permeability of natural materials, in *Flow Through Porous Media,* edited by R. J. M. De Wiest, pp. 53–89, Academic, New York, 1969.

Deju, R. A., *Regional Hydrology Fundamentals,* 204 pp., Gordon and Breach, New York, 1971.

De Wiest, R. J. M. (Ed.), *Flow Through Porous Media,* 530 pp., Academic, New York, 1969.

Fanale, F. P., Martian volatiles: Their degassing history and geochemical fate, *Icarus, 28,* 179–202, 1976.

Gatto, L. W., and D. M. Anderson, Alaskan thermokarst terrain and possible martian analog, *Science, 188,* 255–257, 1975.

Hartmann, W. K., Geological observations of Martian arroyos, *J. Geophys. Res., 79,* 3951–3957, 1974.

Hodgman, C. D., R. C. Weast, and S. M. Selby, *Handbook of Chemistry and Physics,* 39th ed., 3213 pp., Chemical Rubber Company, Cleveland, Ohio, 1957.

Jacob, C. E., and S. W. Lohman, Nonsteady flow to a well of constant drawdown in an extensive aquifer, *Eos Trans. AGU, 33,* 559–569, 1952.

Kliore, A., D. L. Cain, G. S. Levy, V. R. Eshleman, G. Fjelbo, and F. D. Drake, Occultation experiment: Results of the first direct measurement of Mars' atmosphere and ionosphere, *Science, 149,* 1243–1248, 1965.

Latham, G. V., M. Ewing, F. Press, G. Sutton, J. Dorman, Y. Nakamura, N. Toksoz, F. Duennebier, and D. Lammlein, Passive seismic experiment, Apollo 14 Preliminary Science Report, *NASA Spec. Publ., SP-272,* 133–161, 1971.

Leighton, R. B., and B. C. Murray, Behavior of carbon dioxide and other volatiles on Mars, *Science, 153,* 136, 1966.

Lingenfelter, R. E., S. J. Peale, and G. Schubert, Lunar rivers, *Science, 161,* 266–269, 1968.

Malin, M. C., Age of martian channels and nature and origin of intercrater plains on Mars, Ph.D. thesis, Calif. Inst. of Technol., Pasadena, 1976*a*.

Malin, M. C., Age of Martian channels, *J. Geophys. Res., 81,* 4825–4845, 1976*b*.

Masursky, H., An overview of geologic results of Mariner 9, *J. Geophys. Res., 78,* 4037–4047, 1973.

Masursky, H., J. M. Boyce, A. L. Dial, G. G. Schaber, and M. E. Strobell, Formation of Martian channels, *J. Geophys. Res., 82,* 4016–4038, 1977.

McCauley, J. F., Geologic map of the Coprates quadrangle of Mars, *Misc. Map I-897,* U.S. Geol. Surv., Reston, Va., in press, 1979.

McCauley, J. F., M. H. Carr, J. A. Cutts, W. K. Hartmann, H. Masursky, D. J. Milton, R. P. Sharp, and D. E. Wilhelms, Preliminary Mariner 9 report on the geology of Mars, *Icarus, 17,* 289–327, 1972.

McElroy, M. B., T. Y. Kong, and Y. L. Yung, Photochemistry and evolution of Mars' atmopshere: A Viking perspective, *J. Geophys. Res., 82,* 4379–4388, 1977.

Milton, D. J., Water and processes of degradation in the Martian landscape, *J. Geophys. Res., 78,* 4037–4047, 1973.

Milton, D. J., Geologic map of the Lunae Palus quadrangle of Mars, *Map I-894,* U.S. Geol. Surv., Reston, Va., 1974.

Nummedal, D., Fluvial erosion on Mars, paper presented at the Colloquium on Water in Planetary Regoliths, U.S. Army Cold Regions Res. and Eng. Lab., Hanover, N. H., Oct. 5–7, 1976.

Opik, E. J., The martian surface, *Science, 153,* 255–265, 1966.

Owen, T., and K. Biemann, Composition of the atmosphere at the surface of Mars: Detection of argon-36 and preliminary analysis, *Science, 193,* 801–803, 1976.

Peale, S. J., G. Schubert, and R. E. Lingenfelter, Origin of martian channels: Clathrates and water, *Science, 187,* 273–274, 1975.

Phillips, R. J., and R. S. Saunders, The isostatic state of the Martian topography, *J. Geophys. Res., 80,* 2893–2908, 1975.

Pieri, D., Martian channels: Distribution of small channels in the martian surface, *Icarus, 27,* 25–50, 1976.

Pollack, J. B., Climatic change on the terrestrial planets, *Icarus*, in press, 1979.
Robertson, J. B., Digital modeling of radioactive and chemical waste transport in the Snake River Plain aquifer at the National Reactor Testing Station, Idaho, *Open File Rep. IDO-22054*, U.S. Geol. Surv., Reston, Va., 1974.
Salisbury, J. M., The light and dark areas of Mars, *Icarus, 5,* 291–298, 1966.
Samuelson, W. J., Engineering geology of the Norad Combat Operations Center, Colorado Springs, CO, *Eng. Geol., 2,* 20–30, 1965.
Schonfeld, E., Martian volcanism (abstract), *Proc. Lunar Sci. Conf. 8th,* part 11, 843–845, 1977.
Schumm, S. A., Structural origin of large martian channels, *Icarus, 22,* 371–384, 1974.
Sharp, R. P., Mars: Fretted and chaotic terrain, *J. Geophys. Res., 78,* 4073–4083, 1973.
Sharp, R. P., and M. C. Malin, Channels on Mars, *Geol. Soc. Amer. Bull., 86,* 593–609, 1975.
Sharp, R. P., L. A. Soderblom, B. C. Murray, and J. A. Cutts, The surface of Mars, 2, Uncratered terrains, *J. Geophys. Res., 76,* 331, 1971.
Sinton, W. M., and J. Strong, Radiometric observations of Mars, *Astrophys. J., 131,* 459–469, 1960.
Soderblom, L. A., and D. B. Wenner, Possible fossil H_2O liquid-ice interfaces in the martian crust, *Icarus, 34,* 622–637, 1978.
Squyres, S. W., Martian fretted terrain: Flow of erosional debris, *Icarus, 34,* 600–613, 1978.
Thorarinnsson, S., The jokulhlaup from the Katla area in 1955 compared with other jokulhlaups in Iceland, *Misc. Pap. 18,* pp. 21–25, Mus. of Natur. Hist., Reykjavik, Iceland, 1957.
U.S. Geological Survey, Topographic map of Mars, *Misc. Invest. Map I-961,* Reston, Va., 1976.
Wade, F. A., and J. N. de Wys, Permafrost features in the martian surface, *Icarus, 9,* 175–185, 1968.
Wilhelms, D. E., Geologic map of the Oxia Palus quadrangle of Mars, *Map I-895,* U.S. Geol. Surv., Reston, Va., 1976.

(Received June 23, 1978;
revised December 8, 1978;
accepted January 3, 1979.)